CANCER GENOMICS & PROTEOMICS *11*: 217-224 (2014)

Electrophoretic Characterization of the Mammalian Nuclear Matrix Proteome, Nuclear Envelope, Nucleoli and Covalently Bound ADP-Ribose Polymers: Potential Applications to Cancer

XAVIER G. ARANDA[1*], RONALD G. RACHO[2**],
GUSTAVO PACHECO-RODRÍGUEZ[1***] and RAFAEL ÁLVAREZ-GONZÁLEZ[3]

[1]*Graduate School of Biomedical Sciences,*
University of North Texas Health Science Center at Fort Worth, Fort Worth, TX, U.S.A.;
[2]*Texas College of Osteopathic Medicine,*
UNT Health Science Center, Fort Worth, TX, U.S.A.;
[3]*Institute for Cancer Research, University of North Texas System, Fort Worth, TX, U.S.A.*

Abstract. *Background/Aim: Nucleic acid metabolism is biochemically compartmentalized to the nucleus. Thus, it is necessary to define the proteome of the various macromolecular structures within this organelle. Materials and Methods: We isolated the nuclear matrix (NM) fraction from rat liver by sequential centrifugation steps at 13,000 rpm, staggered between endogenous nuclease treatment for 2 h at 37˚C, followed by high-salt (H.S.; 2.0 M NaCl) and non-ionic detergent extractions (0.1%- or 1.0% Triton X-100) to eliminate the bulk of chromosomal DNA/RNA, histone proteins and the nuclear envelope (NE). Results: Integrity of the NM and NE structures was confirmed by electron microscopy. Next, we analyzed the NM proteome on a 20% polyacrylamide gel using the PhastSystem. We observed the absence of histone proteins and the characteristic presence of the lamins by Coomassie blue staining. By contrast, upon silver staining, following electrophoretic separation with a Tris-Borate-EDTA buffer, we observed the NM-associated nucleic RNA and protein-free ADP-ribose polymers. While polymers are found in much lower concentration than RNA in NM, they were purified by affinity chromatography on boronate resin prior to electrophoresis. We observed the electrophoretic resolution of free ADP-ribose chains (5-25 units) by silver staining. Conclusion: The significance of our observations to cancer studies and carcinogenesis is discussed.*

**Present Address:* Department of Biology, University of Texas at Arlington, Arlington, TX, 76019, U.S.A.

***Present Address:* Internal Medicine Residence Program; Mayo Clinic; 4500 San Pablo Road South, Jacksonville, FL, 32224, U.S.A.

****Present Address:* Cardiovascular and Pulmonary Research Branch, National Heart, Lung and Blood Institute, National Institutes of Health, Bethesda, MD, 20892, U.S.A.

Abbreviations: NM, nuclear matrix; NE, nuclear envelope; NPC, nuclear pore complex, L.S., low salt; H.S., high salt; rpm, revolutions per minute.

Correspondence to: Rafael Álvarez-González, Centennial Alumnus of Chemistry/Biochemistry, University of North Texas System, 7617 Ramble Wood Trail, Fort Worth, TX, U.S.A. Tel: +1 8172630205, Fax: +1 8172630205, e-mail: RafaelAlvarez-Gonzalez@my.unt.edu

Key Words: Nuclear matrix, proteomics, electrophoresis, PhastSystem, lamins, histones, poly(ADP-ribose), boronate resin, affinity chromatography, epigenetics, nuclear envelope, nucleoli, chromatin.

The nuclear matrix (NM) is a non-aqueous macromolecular complex of mostly RNA and protein that spans the nucleoplasmic space of eukaryotic cells (1) and provides a rigid scaffold that contributes to the quasi-spherical shape of this prominent cell organelle (2). Even though the nuclear matrix (NM) has not been fully confirmed as a functional biological entity *in vivo* (3), it has been the subject of intense investigation and has been defined as a fixed platform or "scaffold" for the topographical organization of pivotal metabolic chromatin processes such as DNA replication (1, 4, 5), gene expression (1, 6, 7) and DNA repair (1, 8, 9), amongst others. Interestingly, after 30 years of some controversy regarding the actual biological significance of the NM unit *in vivo*, recent microscopic visualization of the nucleoplasmic scaffold has persuaded the scientific community to accept the actual existence of the NM as the architectural skeleton of the cell nucleus (10). Not

surprisingly, it has also recently been identified as a rich source of potentially important cancer protein biomarkers (11) in human neoplasia.

Ever since the first report of NM isolation from rat liver cells by Berezney and Coffey (12), it was clear that this macromolecular structure was made off 98.4% protein, 1.2% RNA, 0.5% phospholipids and 0.1% DNA. In fact, the main polypeptide components of the NM were identified as three abundant acidic proteins with a molecular mass of 60-70 kDa (12). Although this sub-nuclear structure seemed to be always devoid of the bulk of nucleic acids (DNA and RNA), as early as 1979, it was suggested that (13) the NM might be crucial for the control of gene expression.

Regarding the molecular composition of the nuclear scaffold, it has been shown that at least 400 polypeptides are associated with the NM (14). While more than 50% of these proteins may be temporarily associated with this sub-nuclear unit, depending on the stage of the cell cycle, it is now clear that the NM is a significantly dynamic structure that facilitates the proper compartmentalization of the replisome (1, 4, 5), the transcriptome (1, 6, 7) and the repairosome (1, 8, 9).

More importantly, the most prominent molecular components of the NM, namely lamins A, B and/or C, have recently been implicated with specific human diseases, grouped together in a series of pathological anomalies identified as laminopathies (15). This timely report, recently published (15), carefully classified the various mutations that occur in genes encoding the intermediate filament nuclear lamins, as well as associated polypeptides, as they correlate with various pathologies such as cancer, progeria, aging, autosomal dominant Emery-Dreifuss muscular dystrophy, Charcot-Marie-Tooth disease, autosomal dominant leukodystrophy and partial lipodystrophy, *etc*. (15).

Therefore, new rapid and reproducible protocols for the consistent isolation of the nuclear matrix from mammalian tissues are required. Due to the fact that the quantity and identity of proteins co-purifying with the NM fraction varies from cell type to cell type and with the stage of the cell cycle (15, 16), new NM isolation procedures must include a key methodological step that confirms the presence of lamins A, B and C as the markers of this structure, concomitant with the virtual absence of histones, the most abundant proteins typically found in eukaryotic chromatin (7, 17) and which comprise up to 50% of the proteome of the cell nucleus.

Herein, we report the reproducible isolation of the NM fraction from rat liver nuclei, followed by the electrophoretic analysis of the proteome and nucleic acids co-purifying with the NM macromolecular complex, on separate 20% SDS gels using the PhastSystem. We consistently observed a Protein/RNA/poly(ADP-ribose) fraction that predominantly contains the intermediate filament lamins (60-70 kDa), completely free of histone proteins.

Materials and Methods

Materials. Histones and β-NAD+ were purchased from Sigma Chemical Company (St. Louis, MO, USA). Bio-Rex 70, molecular weight markers and 10 X SDS-Tris-Glycine and 10 X Tris-Borate-EDTA stock solutions were obtained from Bio–Rad (Richmond, CA, USA), Pre-casted 20% homogeneous polyacrylamide gels, agarose buffer strips and PhastSystem sample applicators were from GE Healthcare (Piscataway, NJ, USA). All other reagents were reagent grade.

Isolation of nuclei. Rat liver nuclei were obtained from Sprague-Dawley Rats (Charles Rivers Lab, San Diego, CA, USA) and immediately homogenized in a 250 mM sucrose solution containing TKM buffer (50 mM Tris-HCl, pH 7.5 at 4 ˚C; 25 mM KCl and 5 mM $MgCl_2$). The homogenate was filtered through multiple layers of cheesecloth. The mixture collected was further diluted 1:3 (v/v) with 2.3 M sucrose in TKM buffer. Next, the suspension was centrifuged at 39,000 rpm at 0-4˚C. The liver nuclei contained in the pellet were further used as a source for sub-nuclear fractions.

Fractionation of nuclei. Rat liver nuclei were fractionated as previously described (18). Briefly, nuclei were incubated at 37˚C for 2 h to digest the DNA with endogenous nucleases. Nuclei were subsequently centrifuged at 780 x g for 15 min at 4˚C. The pellet was diluted in 10 mM Tris-HCl, pH 7.4 (Buffer A) containing 200 μM $MgCl_2$. Three extractions were carried out with buffer A to remove chromatin DNA. The bulk amount of chromatin remaining, *e.g*., histone proteins, was extracted with buffer A containing 2.0 M NaCl. Next, the NM was obtained by the treatment of the remaining material with 0.1 % Triton X-100, 5 mM $MgCl_2$. After washing the pellet twice in buffer A, containing 5 mM $MgCl_2$ to remove the residual Triton X-100, nuclear matrices were resuspended in buffer A containing 5 mM $MgCl_2$. The different fractions collected were stored at –20˚C until used. The NM fraction was applied to a 20% polyacrylamide gel and electrophoresis was carried out as described below, on the PhastSystem.

Preparation of sub-nuclear samples for electron microscopy. A standard protocol for electron microscopy was followed. First, the samples were fixed overnight with a solution constituted of 2.5% glutaraldehyde in 125 mM PIPES buffer (piperazine-N,N'-bis(2-ethanesulfonic acid)), pH 7.3. In addition, purified nuclei and nuclear matrices also contained buffer A (*vide supra*) with 200 μM $MgCl_2$. Subsequently, samples were post-fixed in 1% OsO_4. Dehydration of the samples was accomplished by a series of treatments with graded ethanol solutions. The fixed material was infiltrated with different ratio mixtures of propylene oxide/epon 812. The samples were then sectioned *via* Leica ultracuts with a diamond knife. Finally, ten and three hundred nanometer sections were stained with orange acetate and Sato's lead. The different sub-nuclear fractions were viewed with a Zeiss EM 910 electron microscope (Zeiss Instruments, Thornwood, NY).

Poly (ADP-ribose) purification. ADP-ribose polymers were purified by affinity chromatography on dihydroxyboronyl-Bio Rex 70 (DHB-B) as described elsewhere (19, 20). Briefly, nuclear matrices containing the NM proteome and nucleic acids were dissolved in 250 mM ammonium formate, pH 9.0 containing 6.0 M guanidine-HCl (10 ml). The samples were loaded onto a 1.0 ml DHB-B

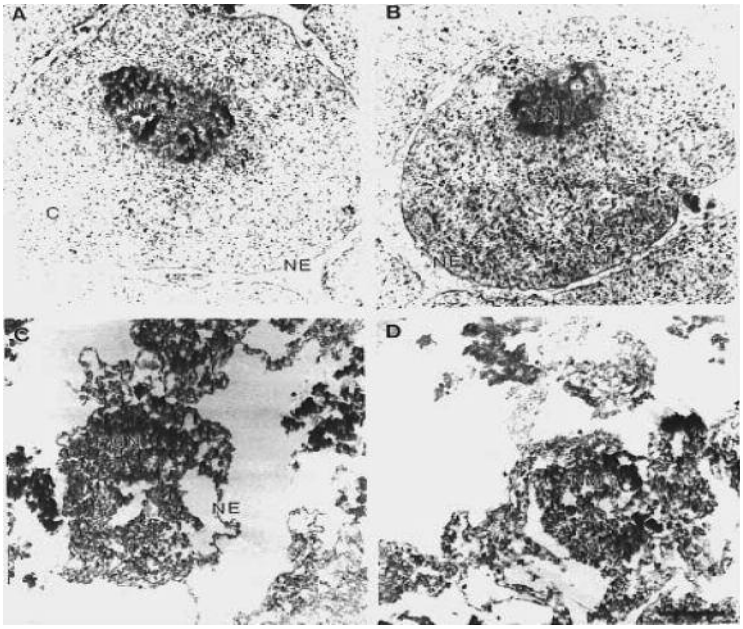

Figure 1. *Electron micrographs of intact rat liver nuclei (panel A), nuclease digested nuclei (panel B), nuclear matrix (NM) with nuclear envelope (NE) (panel C) and NM without NE (panel D). Nuclei (A) were first incubated at 37˚C for endogenous nuclease treatment. The remaining nuclear structure (B) was extracted three times with a low salt buffer and subsequently with 2.0 M NaCl to obtain the structures shown on panel C. Finally, the residual structures were treated with 1.0 % Triton X-100 to obtain the NM without the NE (panel D). Abbreviations: Nu, Nucleolus; NE, nuclear envelope, C, chromatin; and NM, nuclear matrix. Bar=0.97 μm.*

column previously equilibrated with the affinity chromatography loading buffer at 4˚C. Then the column was washed three times with 10 ml of ice-cold 250 mM ammonium formate, pH. 9.0 and the protein-free ADP-ribose polymers were eluted with water at 37˚C. The eluate was lyophilized and used for 20% polyacrylamide gel electrophoresis on the PhastSystem.

Electrophoresis and staining of the NM proteome, nucleic acids and protein-free ADP-ribose polymers. The protein composition of each sub-cellular fraction was first analyzed by SDS-polyacrylamide gel electrophoresis as described by Laemmli (21)Reference) with 0.1% SDS, 12% polyacrylamide (Figure 2) and 4 M Urea. For all other experiments, the nuclear matrix proteins were electrophoresed under SDS-denaturing conditions using pre-casted 20% polyacrylamide gels (GE Healthcare (Piscataway, NJ, USA)) and 50 mM Tris-Glycine buffer, pH 7.8 with the PhastSystem. Separation parameters were as follows: 250 V, 10 mA, 3.0 W, 15˚C, for 90 minutes. Sample loading buffer consisted of 50 mM Tris-Glycine buffer, pH 7.8 from Bio-Rad (Richmond, CA, USA) containing bromophenol blue as a marker and high molecular weight standards, also from Bio-Rad. The gels were fixed in methanol/acetic acid and stained with Coomassie blue for protein. Nucleic acids were also electrophoresed in homogenous 20% polyacrylamide gels and the electrophoresis buffer used was 89 mM Tris-Borate pH 8.3 containing 2.0 mM EDTA. Silver staining for RNA and poly(ADP-ribose) and high specificity was performed according to the commercial specification of the Protostain system from National Diagnostics (Atlanta, GA, USA).

Results and Discussion

Recently, significant interest has been pointed towards the NM proteome as a potential source of cancer biomarkers (10, 16). The rationale is that the mitotic dependence of the NM integrity may be directly involved in the regulation of key cell division metabolic events (15, 16) such as DNA replication (1, 4, 5) or cell cycle-dependent gene expression (1, 6, 7) patterns. At the same time, based on the cell type used as a source for NM purification (13), as well as the actual cell cycle status (220) and, more importantly, the actual protocol of isolation (15, 16), the proteome generated may have varying polypeptide compositions.

For example, while the use of $(NH_4)_2SO_4$ for the high ionic strength extraction of histone proteins may yield a hepatocyte NM proteome with over 500 proteins (16), other methods may result on an average of 400 polypeptides (14). Nonetheless, it must be re-emphasized that, regardless of the NM isolation protocol used, all reports coincide with the conclusion that the most abundant polypeptides in this fraction are lamins A, B or C (1, 13, 14, 16), a class of proteins (23) that belongs to the family of intermediate filament V proteins (23-25). In addition, it must be noted that mutations in the primary sequence of these proteins are

currently associated with NM dysfunctions (13) that may lead to several diseases defined as human laminopathies (15). Therefore, it is clear that all methods of NM isolation must corroborate the presence of the lamins (60-70 kDa) as markers of purity, while the extracts must be devoid of histones (*vide infra*).

Figure 1 displays the morphological integrity of the NM fraction that we isolated from rat liver as described in the Materials and Methods section. Panel A shows the electron microscope structure of intact rat liver nuclei. Panel B shows the morphological appearance of the nuclear product after endogenous nuclease digestion to remove the bulk of DNA. Panel C displays the NM structure still containing the nuclear envelope (NE), after the 2.0 M NaCl extraction of the histone proteins. By contrast, the NM proteome obtained (with small amounts of RNA), after the elimination of the double lipid bilayer with 1.0% Triton X-100, is shown on Panel D. Our morphological results under the electron microscope are identical to NM's isolated from other tissues (11), as well as single cell organisms, such as *Physarum polycephalum* (22).

Figure 2 shows the protein composition of all rat liver nuclei sub-components that were collected during the sub-nuclear fractionation as described above, including the low-salt (L.S.), high-salt (H.S.) and wash solutions. On Figure 2, panel A, lanes1 through 6 display the molecular weight markers (M), isolated nuclei, the endonuclease digestion products and nuclease digested nuclei, low-salt chromatin extract and the Nuclear Matrix I fraction, still containing the NE and all histone proteins, respectively. By contrast, Figure 2-panel B shows in Lanes 1 and 2 the molecular weight markers and an aliquot of intact rat liver nuclei again. Lanes 3 through 7 display the 2.0 M (H.S.) extract, the Nuclear Matrix II (without histone proteins) with NE and Nucleoli, the NE (Triton X-100 Material), the proteins in the washing solution and the purified Nuclear Matrix III (Lamins) that was further processed for the rapid and reproducible 20% polyacrylamide gel analysis using the PhastSystem shown on Figures 3 and 4 below. Interestingly, as shown on panel A, lane 3, most DNA-binding proteins were extracted after the endogenous nuclease digestion of rat liver nuclei. By contrast, the histone proteins were preferentially extracted *via* the L.S. (lane 5, panel A) and H.S. (lane 3, panel B) NM purification steps. Furthermore, the multi-subunit NE complex, as well as integral NE proteins, were extracted with the Triton X-100 step (lane 5, panel B). Thus, as expected, the nuclear matrix III (lane 7, panel B) was almost exclusively constituted of the protein lamins. However, the process of methodological confirmation that the final nuclear matrix proteome was predominantly constituted of histone proteins and completely devoid of histones was both tedious and time consuming. Therefore, we proceeded to speed-up the process of methodological confirmation of these two key

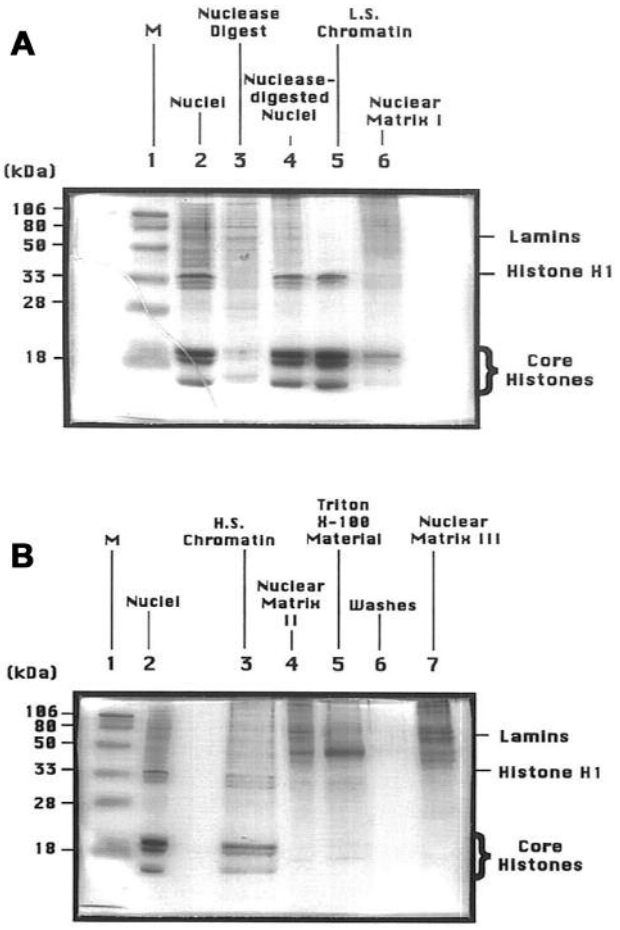

Figure 2. *Proteome (protein composition) of nuclei, nuclear matrix and nuclear envelope (Triton X-100 extract), as determined by Coomassie blue staining following SDS-PAGE. Electrophoresis was carried-out as described under "Materials and Methods". Lane 1 (M) of panels A and B correspond to pre-stained molecular weight markers. The apparent molecular weight of these standards is shown to the left of each panel. The sample applied to each lane is indicated above each lane. Equal amounts of protein (9 μg) were applied per lane.*

molecular parameters using pre-casted and commercially available 2×2 inch 20% polyacrylamide gels and the PhastSystem followed by Coomassie blue staining in less than two hours as shown below.

Figure 3 shows that the main Coomassie blue stained the polypeptides observed, run in the range of 60-70 kDa molecular weight markers, with a 20% polyacrylamide gel under SDS denaturing conditions, which is consistent with the significant abundance of the lamins as markers of NM purity. Lanes 2 and 3 show the lamins just barely migrating 5 mm below the origin due to the high concentration of polyacrylamide (20%). While a few other lower molecular weight proteins, typically associated with the NM fraction,

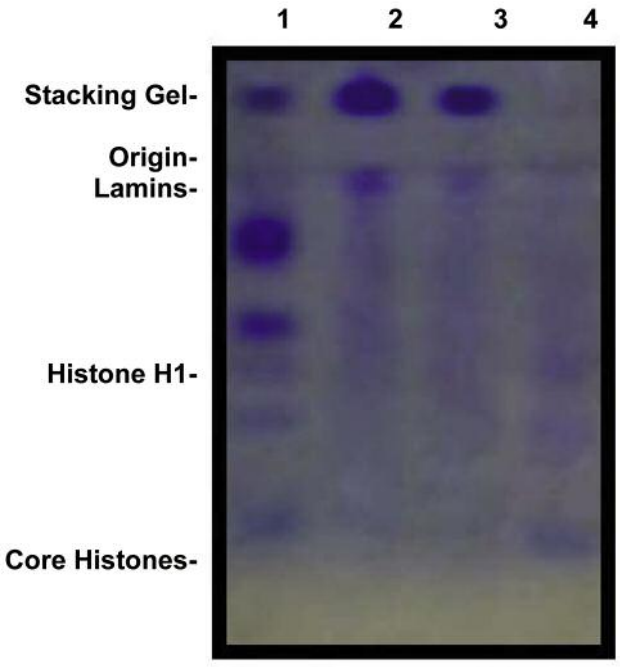

Figure 3. *Electrophoretic separation and identification of the NM lamins following 20% polyacrylamide SDS-PAGE of the NM fraction with the PhastSystem and Coomassie blue staining. Lane 1 shows a sample of high molecular weight markers. Lane 2 shows the rat liver NM fraction. Lane 3 shows the separation of the commercial preparation of histone proteins. Lane 4 shows a mixture of commercial histone proteins.*

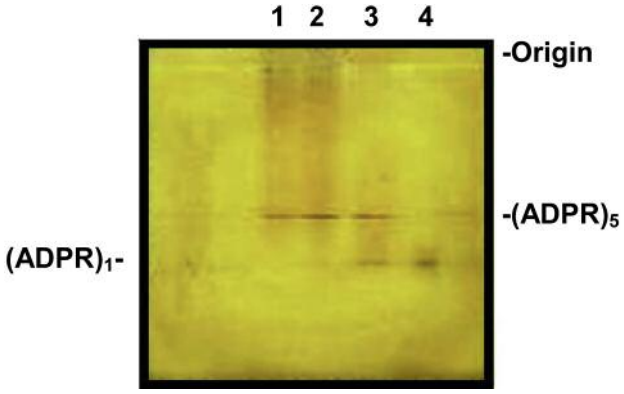

Figure 5. *Electrophoretic identification of the ADP-ribose chains associated with the NM following 20% polyacrylamide TBE-PAGE with the PhastSystem and silver staining. The nuclear matrix (NM) fraction was subjected to affinity chromatography purification on a boronate column, as described in the Materials and Methods section, to eliminate the 1.2% content of RNA. The ADP-ribose chains bound to NM proteins that bind to the boronate were separated on a 20% homogenous polyacrylamide gel with a TBE buffer to facilitate the resolution of short oligomers. Lanes 1 and 2 represent the free ADP-ribose polymers that were obtained from the NM fraction following chemical release during boronate chromatography. Lanes 3 and 4 display the electrophoretic mobility of 50 ng of either a pure ADP-ribose pentamer or a monomer of ADP-ribose, respectively.*

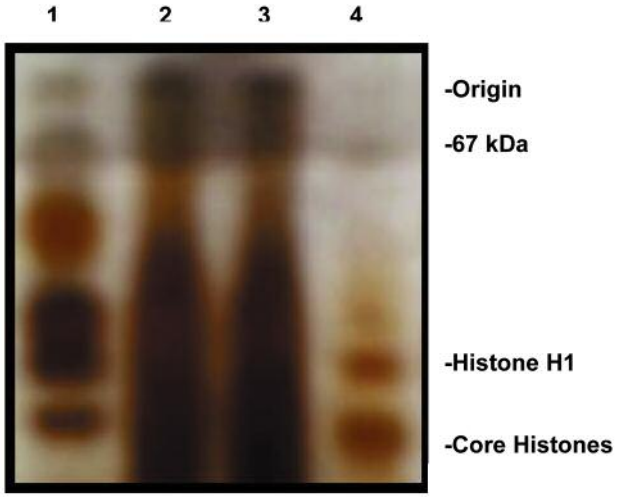

Figure 4. *Composition of the NM proteome and associated nucleic acids (RNA and ADP-ribose polymers) following 20% polyacrylamide SDS-PAGE with the PhastSystem and silver staining. Lane 1 shows the high molecular weight markers. Lane 2 shows the rat liver NM fraction. Lane 3 shows the separation of the commercial preparation of histone proteins. Lane 4 shows a mixture of commercial histone proteins.*

are also present in our samples; their relative abundance is not high enough for Coomassie blue staining. Instead, we clearly observed that all polypeptides with a molecular weight higher than 80 kDa do not migrate into the gel and remain as a single protein band at the origin of the stacking gel. To further confirm the absence of histones, Figure 3-lane 4 shows the expected electrophoretic migration of a mixture of histone H1 and core histones, which are not detectable on lanes 2 and 3. Therefore, in order to further confirm the quantitative removal of histone proteins from the NM by the 2.0 M NaCl extraction (*vide supra*), we run another 20% polyacrylamide gel in parallel, under SDS denaturing conditions as well, but we stained with silver nirate as described in the Materials and Methods section. We observed a smear of silver stained RNA molecules that span the lane completely from the origin of the gel to the bromophenol blue marker at the bottom of the gel (Figure 4, lanes 2 and 3). Lane 4 shows the histone molecular weight markers for comparison.

The presence of a significant amount of silver-stained material is consistent with the presence of short RNA molecules known to be associated with the NM (1-3, 11-13) and perhaps other less abundant nucleic acids, such as the covalently bound ADP-ribose polymers (18, 264) found in the NM. This explanation would also be consistent with the

fact that ADP-ribose chains are chemically released from the protein acceptors by the mild alkaline conditions (27-30) of electrophoresis. Due the importance of the NM in telomere biology (25) and DNA replication (18) and repair (25), we proceeded to seek whether our system would also be useful to determine the size distribution of ADP-ribose polymers (31) in the NM fraction.

Figure 5 shows the silver-stained profile of the ADP-ribose chains co-purifying with the NM proteome after affinity chromatographic purification on DHB-Bio Rex (2019). The free ADP-ribose polymers obtained appear as a smear of silver stained oligonucleotides (Figure 5, lanes 1 and 2) in a region of the electrophoregram that corresponds to ADP-ribose chain lengths oscillating between 5 and 25 ADP-ribose units. Also shown on lanes 1 and 2 is an aliquot of 50 ng ADP-ribose pentamer that was added "to spike" the samples with an internal control for electrophoretic migration reference. Interestingly, using our protocol, we did not see a strong silver band at the origin of the gel, consistent with the notion that no highly branched polymers (31) are synthesized covalently bound to nuclear matrix proteins. Lanes 3 and 4 of Figure 5 show the electrophoretic migration of a pentamer and a monomer of ADP-ribose, respectively.

In conclusion, we have demonstrated that the utilization of homogenous 20% polyacrylamide gels and the PhastSystem can be a useful tool to quickly monitor for the presence of lamins and the absence of histone proteins to confirm the expected protein composition of a nuclear matrix fraction. In addition, we also show that an identical gel can be used to determine the level of NM associated protein-poly(ADP-ribosyl)ation. The presence of these unique polynucleotides, covalently bound to NM protein, becomes even more relevant in light of the recent report of Gonzalez-Suarez *et al*. (25) who demonstrated that the NM is definitely involved in the DNA-damage response pathway and also telomere biology, which eventually connects the NM scaffold as a relevant structure in the early stages of carcinogenesis as suggested by Albrethsen *et al*. (11), as well as Barboro *et al*. (16) (*vide supra*). Likewise the approach described in this report may also become very useful in detailed and careful characterization of the NM, NE and nuleoli proteomic samples acquired from individuals with cancer (11) containing covalently bound modifying groups that alter their overall chemical structure (32) and may epigenetically modify their function. Interestingly, while this study was in the final stages of preparation, a timely report in the Journal of Cell Biology (33) discussed the significance of proteome-bound ADP-ribose polymers in cell and nuclear architecture. In fact, this recent careful analysis confirms previous suggestions (27, 34-36) that the covalent and reversible protein-poly(ADP-ribosyl)ation (37, 38) flows from chromatin and nuclear structures, including the NM (39), to cytoplasmic organelles (35). Similarly, the metabolism in both germ cells (27) and somatic cells (34, 35), including cervical cancer He-La cells, shows re-distribution of ADP-ribose polymers in the nucleoli (36), upon genotoxic damage (40), along with the enzyme (36) responsible for their synthesis (PARP-1) [EC 2.4.2.30]. Interestingly, our observations and interpretations were reproduced 2012 (41) and further confirmed even more recently, in 2014 (33).

Clearly, our understanding over the interplay between the genomics and proteomics of the protein-poly(ADP-ribosyl)ation pathways in human cells shall prove instrumental in the diagnosis, prognosis and treatment of cancer.

References

1 Zeits MJ, Malyavantham KS, Seifert B, and Berezney R: Matrin 3: Chromosomal distribution and protein interactions. J Cell Biochem *108*: 125-133, 2009.

2 Rowat AC, Lammerding J, Herrmann H, and Aebi U: Towards and integrated understanding of the structure and mechanics of the cell nucleus. BioEssays *30*: 226-236, 2008.

3 Nickerson J: Experimental observations of a nuclear matrix. J Cell Sci *114*: 463-474, 2001.

4 Courbet Gay S, Arnoult N, Wronka G, Anglana M, Brison O and Debatisse M: Replication fork movement sets chromatin loop size and origin choice in mammalian cells. Nature (London) *405*: 557-560, 2008.

5 Shaman JA, Yamauchi Y and Ward WS: The sperm nuclear matrix is required for paternal DNA replication. J Cell Biochem *102*: 680-688, 2007.

6 Razin SV, Iarovala OV, Sjakste N, Sjakste T, Bagdonieri L, Rynditch AV, Elvazova ER, Lipinski M and Vassetsky YS: Chromatin domains and regulation of transcription. J Mol Biol *369*: 597-607, 2007.

7 Shimi T, Pfleghaar K, Kojima S, Pack CG, Solovel I, Goldman AI, Adam SA, Shumaker DK, Kinjo M, Cremer Tand Goldman RD: The A- and B-type nuclear lamin networks: microdomains involved in chromatin organization and transcription. Genes Dev *22*: 3409-3421, 2008.

8 Roti Roti JL: Heat-induced alterations of nuclear matrix protein-associations and their effects on DNA repair and replication. Int J Hyperthermia *23*: 3-15, 2007.

9 Atannasov B, Gospodinov A, Stoimenov I, Mladenov E, Russev G, Tsaneva I and Anachkova B: Repair of DNA interstrand crosslinks may take place at the nuclear matrix. J Cell Biochem *96*: 126-136, 2005.

10 Elcock LS and Bridger JM: Exploring the effects of a dysfunctional nuclear matrix. Biochem Soc Transactions *36*: 1378-1383, 2008.

11 Albrethsen J, Knol JC and Jimenez CR: Unraveling the nuclear matrix proteome. J Proteomics *72*: 71-81, 2009.

12 Berezney R and Coffey DS: Identification of a nuclear protein matrix. Biochem Biophys Res Commun *60*: 1410-1417, 1974.

13 Shaper JH, Pardoll DM, Kauffmann SH, Barrack ER, Vogelstein B and Coffey DS: The relationship of the nuclear matrix to cellular structure and function. Adv Enzyme Regul *17*: 213-220, 1979.

14 Mika S and Rost B: NMPdb: database of nuclear matrix proteins. Nucleic Acids Res *33*: D160-D163, 2005.

15 Worman WJ and Bonne G: "Laminopathies": a wide spectrum of human diseases. Exp Cell Res *313*: 2121-2133, 2005.
16 Barboro P, Repaci E, D'Arrigo C and Balbi C: The role of nuclear matrix binding to matrix attachment regions (Mars) in prostate cancer cell differentiation. PLos One *7*: e40617, 2012.
17 Hansen JC, Lu X, Ross EDand Woody RW: Intrinsic protein disorder, amino acid composition and histone terminal domains. J Biol Chem *281*: 1853-1856, 2006.
18 Ávarez-González R and Ringer DP: Nuclear matrix associated Poly(ADP-ribose) metabolism in regenerating rat liver. FEBS letters 236: 362-366, 1988.19 Álvarez-González R, Juárez-Salinas H, Jacobson EL and Jacobson MK: Evaluation of immobilized boronates for studies of adenine and pyridine nucleotide metabolism. Analytical Biochem *136*: 69-77, 1983.
20 Alvarez-Gonzalez R, Eichenberger R, Loetscher P and Althaus FR: A new highly selective physicochemical assay to measure NAD+ in intact cells. Analytical Biochem *156*: 473-480, 1986.
21 Laemmli UK: Cleavage of structural proteins during the assembly of the head of bacteriophage T4". Nature *227*: 680-685, 1970.
22 Lang S, Decristoforo T, Waitz Wand Loidl, P: Biochemical and morphological characterization of the nuclear matrix during the synchronous cell cycle of *Physarum polycephalum*. J Cell Sci *105*: 1121-1130, 1993
23 Ben-Harush K, Wiesel N, Frenkiel-Krispin D, Moeller D, Soreq E, Aebi U, Herrmann H, Grauenbaum Y and Medalia O: The supramolecular organization of the C. elegans nuclear lamin filament. J Mol Biol *386*: 1392-1402, 2009.
24 Herrmann H, Barr H, Kreplak L, Strelkov SV and Aebi U: Intermediate filaments: from cell architecture to nanomechanics. Nature Reviews Mol Cell Biol *8*: 562-573, 2007.
25 Gonzalez-Suarez I, Redwood AB, Perkins SM, Vermolen B, Lichstensztejin D, Grotsky DA, Morgado-Palacin L, Gapud EJ, Sleckman BP, Sullivan T, Sage J, Stewart CL, Mai S and Gonzalo S: Novel roles for A-type lamins in telomere biology and the DNA damage response pathway. EMBO J *28*: 2414-2427, 2009.
26 Cardenas-Corona ME, Jacobson EL and Jacobson MK: Endogenous polymers of ADP-ribose are associated with the nuclear matrix. J Biol Chem *262*: 14863-14967, 1987.
27 Atorino L, Álvarez-González R, Cardone A, Lepore I, Farina B and Quesada P: Metabolic changes in the Poly(ADP-ribosyl)ation) Pathway of differentiating rat germinal cells. Arch Biochem Biophys *381*: 111-118, 2000.
28 Mendoza-Álvarez H, Chávez-Bueno S and Álvarez-González R: Chain length analysis of ADP-ribose polymers generated by poly(ADP-ribose) polymerase (PARP) as a function of beta-NAD+ and enzyme concentrations. IUBM Life *50*: 145-149, 2000.
29 Mendoza-Álvarez H and Álvarez-González R: Regulation of p53 sequence-specific binding by covalent poly(ADP-ribosy)ation. J Biol Chem *276*: 36,425-36,430, 2001.
30 Confer NF, Kumari SR and Álvarez-González R: Biochemical association of Poly(ADP-ribose) polymerase-1 and its apoptotic peptide fragments with DNA polymerase beta. Chemistry and Biodiversity *1*: 1476-1486, 2004.
31 Álvarez-González R and Jacobson M: Quantification of poly(ADP-ribose) in vitro: Determination of Chain Length and Branching Pattern. Methods in Molecular Biology *780*: 35-46, 2011.
32 Simon DL and Wilson KL: Partners and post-translational modifications of nuclear lamins. Chromosoma *122*: 13-31, 2013.
33 Leung AKL: Poly(ADP-ribose) and organizer of cellular architecture. J Cell Biol *205*: 613-619, 2014.
34 Alvarez-Gonzalez R, Eichenberger R, Loetscher P and Althaus FR: A new highly selective physicochemical assay to measure NAD+ in intact cells. Analytical Biochem *156*: 473-480, 1986.
35 Loetscher P, Alvarez-Gonzalez R and Althaus FR: Poly(ADP-ribose) may signal changing metabolic conditions to the chromatin of mammalian cells. Proceedings of the National Academy of Sciences (USA) *84*: 1286-1289, 1987.
36 Alvarez-Gonzalez R, Spring H, Müller M and Bürkle A: Selective loss of poly(ADP-ribose) and the 85-kDa Fragment of poly(ADP-ribose) polymerase in nucleoli during alkylation-induced apoptosis of HeLa cells. J Biol Chem *274*: 32122-32126, 1999.
37 Alvarez-Gonzalez R: Poly(ADP-ribosyl)ation of chromosomal proteins, epigenetic regulation and human genomic integrity in Health and Disease. Protein Reviews *13*: 411-424, 2010.
38 Alvarez-Gonzalez R, Mendoza-Alvarez H, Frey M and Zentgraf H: Up-regulation of two distinct p53-DNA binding functions by covalent poly(ADP-ribosyl)ation: transactivation and single strand break sensing. Cancer Investigation *31*: 563-570, 2013.
39 Pacheco-Rodriguez G and Alvarez-Gonzalez R: Measurement of poly (ADP-ribose) glycohydrolase activity by high resolution polyacrylamide gel electrophoresis: specific inhibition by histones and nuclear matrix proteins. Mol Cell Biochem *193*: 13-18, 1999.
40 Kumari SR and Alvarez-Gonzalez R: Expression of c-jun and c-fos in apoptotic HeLa cells following DNA-damage. Cancer Investigation *18*: 715-721, 2000.
41 Boamah EK, Kotova E, Garabedian M, Jarnik M and Tulin AV: Poly(ADP-ribose) Polymerase I (PARP-1) regulates ribosomal biogenesis in Drosophila Nucleoli. PLoS Genet *8*: e1002442, 2012.

Received July 10, 2014
Revised August 4, 2014
Accepted August 6, 2014